The Fast Photorefractive Effect and Its Application to Vibrometry

Russell M. Kurtz,[1,*] Weixing Lu,[1] Judy Piranian,[1]
Tomasz Jannson,[2] and Albert O. Okorogu[3]

[1]RAN Science & Technology, LLC, 2101 Via Rivera, Palos Verdes Estates, CA 90274, USA
[2]Physical Optics Corp.,20600 Gramercy Pl., Torrance, CA, USA
[3]The Aerospace Corporation, P.O. Box 92957, Los Angeles, CA 90009, USA

We previously reported[1] on what we describe as the "fast photorefractive effect," photorefractive signal amplification at much greater frequencies than predicted by its grating formation speed. In this paper we explain the effect and its potential for application to vibrometry. We demonstrated photorefractive amplification in Cu:KNSBN (whose grating formation speed is <5 Hz), matching the standard model with CW illumination. We then demonstrated photorefractive amplification of vibrometric signals at frequencies up to 4 MHz. Our theory of the fast photorefractive effect indicates that the amplification bandwidth of Cu:KNSBN at 488 nm illumination could exceed 800 GHz.

Keywords: Fast Photorefractive Effect, Photorefractivity, Vibrometry, Cu:KNSBN, Long-Range Detection

1. INTRODUCTION

Photorefractive amplification has a number of advantages as part of a vibrometric detection system. It provides significant amplification (>20 dB) in a narrow bandwidth (<1 nm), resulting in significant enhancement of the signal-to-noise ratio (SNR). It is easy to set up, adaptable to many real-life situations, and can be used over a wide spectral range with little modification. It has the disadvantage, however, of being a slow process;[2] response bandwidth is rarely greater than ~100 Hz. Under certain conditions, however, photorefractive amplification occurs over a much larger bandwidth. These conditions include measuring the motion of a target illuminated by a CW laser[1] and situations in which the photorefractive grating is independent of the signal.[3] Our experiments demonstrated photorefractive amplification of signals with bandwidth >2 MHz, limited by our equipment, and calculations indicate amplification of signals centered at 488.0 nm with bandwidths up to 832 GHz, all in Cu:KNSBN, which has a photorefractive grating response bandwidth <5 Hz.

2. THEORY

Theory of the fast photorefractive effect is based on both photorefractive theory and vibrometric theory. The photorefractive theory begins with the Standard Photorefractive Model (STPM).[4]

2.1 Photorefractivity – The Standard Model

Photorefractivity is the result of space charge displacement in media that have a large electro-optic effect. These displaced charges result in a large internal field, which creates a refractive index modulation due to the nonlinear effect. In many cases, the internal electric field is limited only by the diffusion field. Then, if the illumination is modulated sinusoidally by interference between two beams, the space-charge field will also be sinusoidal, and will be shifted by 90° with respect to the illumination. This results in maximum power transfer from one beam to the other (which gains power and which loses it depends on the relative polarizations of the beams, the sign of the electro-optic coefficient, and the direction of the *c*-axis of the medium).

The STPM models a photorefractive medium as a type of doped semiconductor. The host medium is transparent at the illumination wavelength. The dopant absorbs strongly at that wavelength. In this situation, the bandgap of the dopant is less than that of the host, so it adds additional effective energy levels to the medium. When a photon enters the medium, it ionizes the dopant, moving an electron into the host conduction band. This electron then gives up a small amount of energy, ending in a trap level at or near the conduction band energy of the dopant, but below the conduction band energy of the host (Fig. 1).
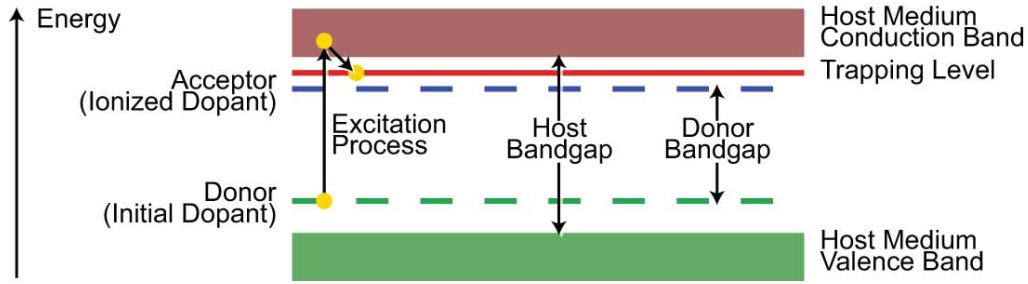
RESEARCH ARTICLE

Fig. 1. Photoexcitation of an ion in a photorefractive material requires photon energy great enough to ionize the dopant, but small enough to avoid ionization of the host.

The electron in the trapping level may then move due to diffusion, or be moved by an applied electric field. If it ends up in an area where there is a considerable amount of light, it is likely to be knocked out of the trapping level and back to the valence band of the dopant by stimulated deexcitation. If the electron ends up in a dark location, its probability of deexcitation is much lower; it can only return to its valence band spontaneously, with probability depending on the ratio of available thermal energy to the energy needed to deexcite the electron [$k_B T/(E_{gd} + E_{gh} − E_t)$, where k_B is Boltzmann's constant, T is the local temperature in absolute units, E_{gd} is the dopant bandgap energy, E_{gh} is the host bandgap energy, and E_t is the energy of the trapping level]. In many photorefractive materials, particularly those excited by visible light (*e.g.* $BaTiO_3$, SBN, $LiNbO_3$), this can be very slow. The probability density of spontaneous emission at room temperature is approximated in Figure 2 as a function of the long-wave cutoff wavelength of the dopant in the host medium.

Since the electrons congregate in the dark areas and flee the illuminated areas, if the photorefractive medium is illuminated by an interference pattern, the internal space-charge field will also be repetitive. The layout of such a situation, with the two beams that form the interference pattern both linearly polarized in the plane of incidence, is shown in Figure 3.
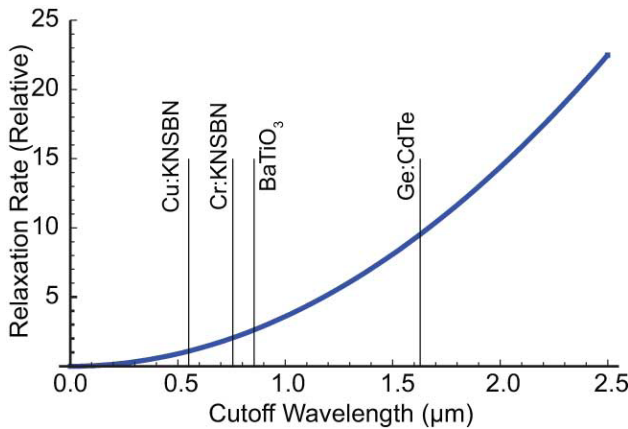

Fig. 2. The approximate deexcitation probability of photorefractive Ge:CdTe is 9× as great as that of Cu:KNSBN at room temperature.

In the layout described by Fig. 3, the contrast of the interference pattern is

$$m = 2\frac{\sqrt{I_0 I_1}}{I_0 + I_1}\cos(2\theta) \tag{1}$$

If the photorefractive medium is limited by diffusion, and the medium is both insulated and a good insulator, the STPM tells us that the long-term space-charge field will be

$$E_{sc} = \frac{k_B T k \cos\theta}{q}\sin(2\pi x/\Lambda + \varphi) \tag{2}$$

where k is the propagation vector of I_0 and I_1, q is the magnitude of the electron charge, and φ is a phase constant selected so that the intensity of the interference pattern is $I_{ip} = I_{max}\cos(2\pi x/\Lambda + \varphi)$. The build-up to this final field is exponential; its time dependence is

$$E_{sc}(x,t) = E_{sc}(x,\infty)\left(1 - \exp\left\{\left[\sigma I(x)\lambda/hc - \gamma_R\right]t\right\}\right) \tag{3}$$

where σ is the absorption cross-section of the dopant at the wavelength of the illumination, $I(x)$ is the total illumination at position x, and γ_R is the recombination (or spontaneous emission) rate for trapped electrons. Equation (3) also shows that, for the modulated field to form at all, the total illumination must satisfy $I_0 + I_1 > hc\gamma_R/\lambda\sigma$. Since γ_R increases both with long cutoff wavelength of the dopant and with grating formation speed of the photorefractive material, faster photorefractive materials require
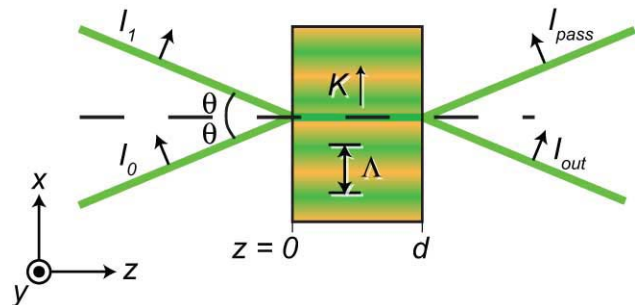

Fig. 3. If the two illumination beams are incident on the medium at the same angle with respect to the *z*-axis, the resulting interference pattern gradient is along the *x*-axis.

stronger beams to generate the internal field. Longer wavelength operation also requires higher power, but the effect is less strong than the grating formation speed effect.

   Now that we know the electric field, we can calculate the refractive index change caused by the first-order electro-optic effect. In the layout of Figure 3, the internal field is directed only along *x*. If the *c*-axis of the medium is also aligned with the *x*-axis, the refractive index change caused by the space-charge field is

$$\Delta n_e = -\frac{1}{2} r_{33} n_e^3 E_{sc} = -\frac{k_B T k r_{33} n_e^3 \cos\theta}{2q} \sin(2\pi x / \Lambda) \quad (4)$$

where r_{33} is the linear electro-optic coefficient for light polarized along the medium's *c*-axis, caused by an electric field directed along this axis; n_e is the refractive index of the extraordinary ray (polarized along the *c*-axis of the medium); and φ has been set to 0 by selection of the origin.

   The photorefractive medium can now be described as a transparent medium with a sinusoidal index variation. Under the assumptions that $\Delta n_e \ll n_e$ and that the medium is not optically active, Kogelnik's theory of volume Bragg gratings[5] enables calculation of the photorefractive grating diffraction efficiency:

$$\eta_{pr} = \sin^2 \left(\frac{\pi d}{\lambda} \frac{\cos 2\theta}{\cos\theta} \Delta n_e \right)$$
$$= \sin^2 \left[\frac{2\pi^2 d k_B T r_{33} n_e^3 \cos 2\theta}{2q\lambda^2} \sin\left(\frac{4\pi x \cos\theta}{\lambda} \right) \right] \quad (5)$$

where Δn_e is calculated from Eq. (4) and, as shown in Figure 3, thickness of the photorefractive medium is *d*. The grating spacing has been calculated from

$$\Lambda = \frac{\lambda}{2\cos\theta} \quad (6)$$

The photorefractive diffraction efficiency defines the limit of how much light can be diverted from one beam into the other. The raw gain factor of the photorefractive grating, assuming no absorption in the host, is

$$g_{pr} \equiv \frac{I_{out}}{I_0} = 1 + \sin^2 \left(\frac{\pi^2 k_B T r_{33} n_e^3 \cos 2\theta}{\lambda^2 q} d \right) \Big/ \left(1 - \sqrt{1 - m^2} \right)^2 \quad (7)$$

As an example, assume we are using Cu:KNSBN, whose extraordinary refractive index is 2.33 and whose relevant electro-optic coefficient is $r_{33} = 270$ pm/V. Operating at room temperature, with 488-nm illumination beams meeting at 45°, the amplification can exceed 80 dB (Figure 4).

2.2 Vibration Detection

We have seen that a photorefractive medium provides excellent gain, if the interference pattern contrast and medium thickness are selected properly. To use this material in a vibrometer, however, it is necessary to determine
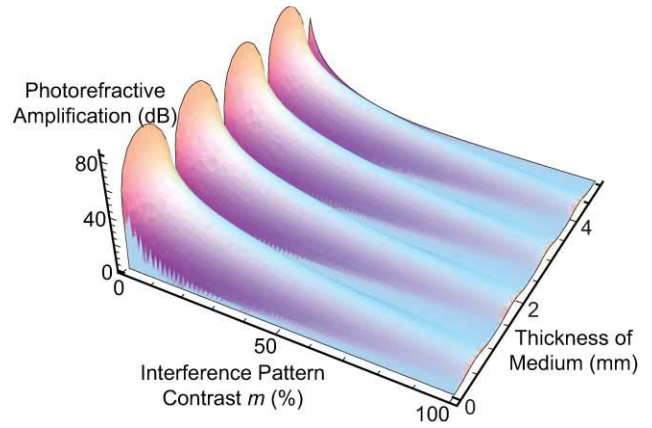
Fig. 4. The photorefractive amplification depends sinusoidally on medium thickness and inversely on contrast.

how it will respond to a signal reflected from a vibrating target (Figure 5).

   The vibrating target changes the overall path length of the beam by $2\Delta z(t)$. (Photorefractive amplification is an interferometric measurement technique, so only axial motion—described here as motion along the *z* axis—is measured. Transverse motion does not affect the path length, so it is not detected by the fast photorefractive effect.) Assuming the distance z_0 to be much greater than the distance between the illumination and the reception, we can ignore angular propagation effects. Then if the illumination $E(z, t)$ is a plane wave traveling in the $+z$ direction, the reflected beam can be written

$$E_R(z,t) = E_I e^{-i[\omega t + kz + 2k\Delta z(t)]} = E_I e^{-i(\omega t + kz)} e^{i2k\Delta z(t)} \quad (8)$$

In other words, the reflected beam is the exact beam that would be expected from a stationary target, multiplied by the phase factor $e^{i2k\Delta z(t)}$. Note that this is different from a pure frequency shift; essentially, instead of changing ω into $\omega + \Delta\omega$, the vibration has changed *z* into $z + \Delta z$. Vibrometry includes the need to determine the frequency components of the measured vibration; to determine the frequency components of $e^{i2k\Delta z(t)}$ we first take the Fourier decomposition of the vibration itself:

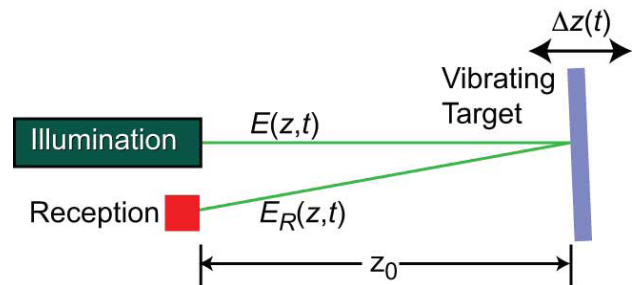$$\Delta z(t) = \sum_{n=-\infty}^{\infty} a_n e^{i2\pi n \nu_0 t} \quad (9)$$

Fig. 5. The vibrating target imposes a phase modulation on the reflected **beam.**

where ν_0 is the frequency of the complete vibrational signal. Using Eq. (9), and remembering that the motion must be real, we can write the phase factor as

$$e^{-i2k\Delta z(t)} = \exp\left[-i2k\sum_{n=-\infty}^{\infty} a_n \cos(2\pi n\nu_0 t)\right]$$
$$= \prod_{n=-\infty}^{\infty} e^{-i2ka_n \cos(2\pi n\nu_0 t)} \quad (10)$$

Each Fourier component, then, has amplitude $2ka_n$. For each Fourier component we use Jacobi-Anger expansion:

$$e^{-i2ka_n \cos(2\pi n\nu_0 t)} = \sum_{m=-\infty}^{\infty} (-1)^m J_{2m}\left(-2ka_n\right) e^{i4\pi mn\nu_0 t} \quad (11)$$

where $J_m(z)$ is the mth-order Bessel function of the first kind evaluated at z. We first consider the Fourier component at no frequency shift, $n = 0$.

$$e^{-i2ka_n \cos(2\pi n\nu_0 t)}\bigg|_{n=0} = e^{-i2ka_0} \quad (12)$$

So this component, as expected, does not vary with time. Nonetheless, *regardless of vibrational frequency* ν_0, there is a signal at zero frequency shift. By the selection of z_0 we ensured that $\Delta z(t)$ is even, so $a_0 = 0$ and the zero-frequency component is just 1, and the exponentials of the $\pm m$ orders add to cosine functions. Thus, for $n = \pm 2$ ($a_{-1} = a_1 = 0$) the phase factor is

$$e^{i2ka_1 \cos(4\pi m\nu_0 t)} + e^{-i2ka_{-1}\cos(-4\pi m\nu_0 t)}$$
$$= 2J_0(0) + 4\sum_{m=1}^{\infty} J_{2m}\left(-2ka_1\right)\cos\left(4\pi m\nu_0 t\right) \quad (13)$$

This balancing of the n with the $-n$ component continues for all $n > 0$. But the peak value of the Bessel function $J_m(z)$ drops exponentially with $|m|$ and inversely with $|z^{1/2}|$, so we can limit ourselves to values $m = 0$ and ± 1, and to the first few values of n (at least for vibration amplitudes on the order of an illumination wavelength). Indeed, a typical vibrational signal will have only a few frequency components; typically

$$e^{i2k\Delta z_0(t)} \approx e^{-i2ka_1 \cos(4\pi m\nu_0 t)} + e^{-i2ka_{-1}\cos(-4\pi m\nu_0 t)}$$
$$= 3 + 4J_2\left(-2ka_1\right)\cos\left(4\pi\nu_0 t\right) \quad (14)$$

is a sufficiently accurate approximation to the vibrational signal. The two important points are: (1) there is a reflected signal at no frequency shift, containing about half the total power; and (2) there is another signal at twice the vibration frequency, containing most of the rest of the power. Since the reflected beam has a large component at zero frequency shift—in other words, at the same exact wavelength as the illuminating beam—a static photorefractive grating is formed. The fast photorefractive effect is the diffraction of the frequency-shifted component from this stationary photorefractive grating. Since there is no need to form a

grating at the difference frequency, the grating formation time does not limit the amplification bandwidth, as would be the case if the reflected beam had a pure frequency shift, instead of a phase modulation.

The reflected signal can be recovered through heterodyne or homodyne detection. Homodyne detection involves mixing it with a portion of the illumination beams to generate a signal at the beat frequency. If these two beams are mixed in a photorefractive crystal, the zero-shift component of the reflected signal will interfere with the outgoing beam to create a stable interference pattern. This creates a sinusoidal index variation in space, which the frequency-shifted portion of the beam will then use for photorefractive amplification. Thus, despite the low speed of setting up the photorefractive grating, relatively high vibrational frequencies can still be amplified.

2.3 Amplification Bandwidth and Angular Acceptance

The photorefractive grating can be described in terms of phase or refractive index. In the diffusion limit, as described above, the refractive index is modulated sinusoidally and $\Delta n \ll n$. This meets all Kogelnik's approximations for volume Bragg gratings and the two beams at the same frequency are automatically at the Bragg angle with respect to the photorefractive grating. We have assumed so far that these beams are plane waves. If one of the beams is expanding or focusing, however, it is not quite a plane wave. This can happen, for example, when the reflected signal is collected by a telescope to increase its intensity prior to its being directed into the photorefractive medium. If the beam has some divergence or convergence angle $\Delta\theta$, Eq. (7) becomes

$$g_{\text{pr}} = 1 + \frac{1}{\left(1 - \sqrt{1 - m^2}\right)^2} \frac{\Delta n^2}{\Delta n^2 + \Delta\theta^2 \tan^2 2\theta}$$
$$\times \sin^2\left(\frac{\pi d}{\lambda \cos\theta}\sqrt{\Delta n^2 \cos^2 2\theta + \Delta\theta^2 \sin^2 2\theta}\right) \quad (15)$$

where Δn is the Δn_{e} of Eq. (4). The acceptance angle is $\Delta\theta \approx \Delta n$. With the model used to produce Figure 4, the acceptance angle is 1.9 arc minutes (0.52 mr). If the beam is a plane wave, the amplification bandwidth can be calculated instead. For this example, $d\theta/d\lambda \approx 0.385/\lambda$, so $\Delta\lambda \approx 0.660$ nm ($\Delta\nu \approx 832$ GHz). In other words, when a photorefractive amplifier with the characteristics described here is used to detect signals, its amplification bandwidth is ~0.66 nm (0.14% of the illumination wavelength) and it can detect vibration signal frequencies as large as >800 GHz. Note also that the narrow passband of the photorefractive amplifier enables it to act as a filter, passing <0.15% of the background together with 100% of the signal for a potential SNR improvement up to 48 dB.

3. EXPERIMENT AND DISCUSSION

We tested a photorefractive crystal, Cu:KNSBN, under illumination at 488.0 nm from a single-frequency argon laser. Its linewidth was sufficiently narrow to ensure that all beams in the experiment were mutually coherent. The crystal chemistry was studied by electron diffraction spectroscopy at the University of California, Irvine, spectroscopy facility, and determined to have the formula $(K_{0.45}Na_{0.55})_{0.16}(Sr_{0.78}Ba_{0.22})_{0.92}Nb_2O_6$. This is a slight variation from the standard KNSBN formula of $(K_{0.5}Na_{0.5})_{0.2}(Sr_{0.75}Ba_{0.25})_{0.9}Nb_2O_6$,[6] but the crystal performed as we would expect from Cu:KNSBN. We measured the refractive indices at 488.0 nm to be n_e = 2.33234±0.00558 and n_o = 2.38091±0.01851. The linear electro-optic coefficients are r_{13} = 50 pm/V, r_{42} = 400 pm/V, and r_{33} = 270 pm/V.[7] We measured the mass density of the crystal to be 6.33 g/cm³. The Cu doping was nominally 0.04% by weight (meaning 0.04% by weight of CuO added to the mixture that makes KNSBN); this corresponds to Cu^+ ion density of $1.92{\times}10^{19}$ cm⁻³. The crystal measured 4 mm × 5 mm × 6 mm, with its *c*-axis along the 6-mm length. All experiments were performed at controlled room temperature, 297K.

The experimental layout is shown in Figure 6. Each beam made an angle of $\pi/8$ (22.5°) with the normal to the crystal face. The beams were polarized in the plane of incidence, resulting in a photorefractive grating whose gradient was in the same direction as the crystal optical axis. The intensity of the reference beam, I_0, was 8.15 W/cm² and that of the signal beam, I_1, was 97.8 mW/cm². The expected interference pattern contrast, then, was 0.2.

Given the relevant parameters—n_e = 2.33234, r_{33} = 270 pm/V, T = 297K, λ = 488.0 nm, θ = 22.5°, m = 0.216, and d = 4.00 mm—we expect single-pass amplification of ~35 for the beam without frequency shifting. Our measurements showed steady-state amplification of 33.5, well within the experimental error. When we blocked the reference beam (I_0), then observed the output (I_{out}) as we unblocked the reference, we determined that the amplification had a response time of 0.2323 s (from 0 to 1–1/*e* of final output). From this we estimated that, with total input intensity $I_0 + I_1$ = 8.25 W/cm², amplification
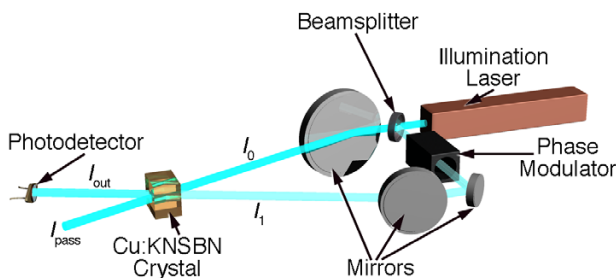
of signals with frequencies slightly different from that of the reference would have a bandwidth of 4.305 Hz.

We then tested the response with the phase modulator set to a sawtooth wave, with retardation changing linearly from 0 to 2π. If the repetition rate of the sawtooth is $\Delta\nu$, this phase modulation is exactly the same as a pure frequency shift of $\Delta\nu$. We ran a logarithmic sweep from $\Delta\nu$ = 0 to 20 Hz. The amplification of this system matched the exponential model to an accuracy of 98.6% (Figure 7(a)).

If we consider the amplified signal beam (I_{out}) to consist of "information" on top of a "carrier," the "information" signal will be the portion of the amplified signal at the modulation frequency (red line in Figure 7(b)). The "information" bandwidth of our photorefractive amplifier was ~5 Hz, although there was sufficient random noise that we estimate its actual bandwidth to be the same as that of the "carrier" (red line in Figure 7(a)). At 10 Hz, the "information" amplitude has dropped to <25% of its dc value; by 20 Hz it has dropped to <15%.

We then repeated the experiment, but instead of using a sawtooth wave to drive the phase modulator we used a sine wave. Thus, instead of a frequency shift, we generated a pure phase shift. This phase shift is predicted to generate mainly two Fourier components: one at zero frequency shift and the other at $2\Delta\nu$, each with about half the
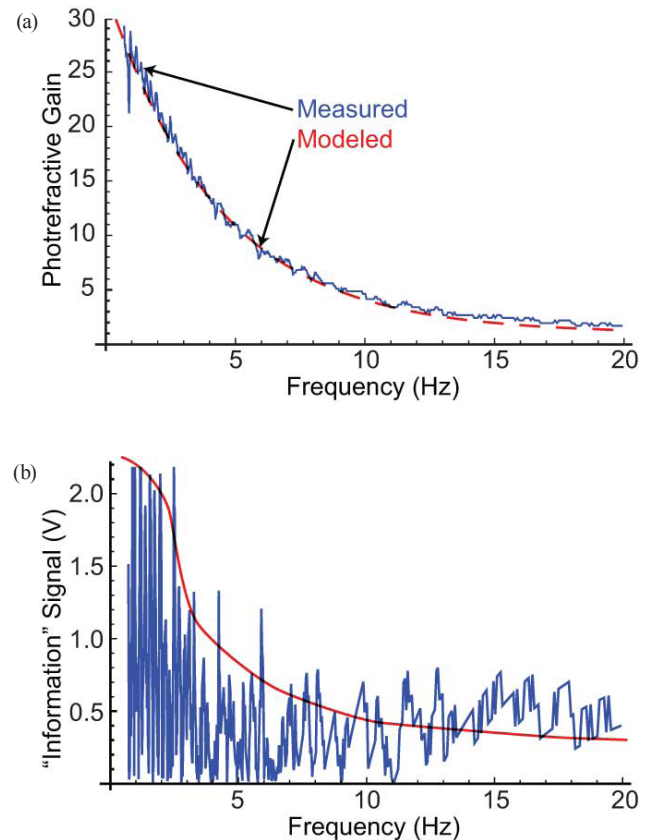
(a)

(b)

Fig. 7. (a) Photorefractive amplification, as a function of frequency difference between the beams, had a bandwidth of 4.3 Hz. (b) The "information" portion of the signal had a bandwidth somewhat larger, ~5 Hz.

Fig. 6. The Cu:KNSBN test was performed at an illumination wavelength of 488.0 nm.

power. The zero-shift component of the signal beam should interfere with the reference beam to produce a photorefractive grating, and the shifted component should be amplified approximately the same amount across the frequency sweep. We predicted a drop in "carrier" amplification but not in "information" amplification. Since the "information" also participated in the photorefractive grating, we predicted a wider bandwidth for the "carrier" as well. This experiment validated our predictions (Fig. 8).

The parameters of this experiment, assuming diffusion limit, indicate that the internal electric field amplitude is $E_{sc} = 3.57$ V/cm, resulting in a refractive index modulation of 5.215×10^{-4}. The Kogelnik model predicts an acceptance angle of 1.79 arc minutes, wavelength acceptance of 0.661 nm, and amplification bandwidth of 832 GHz. This was far beyond our measurement capabilities. In a previous work,[1] we demonstrated large photorefractive gain for phase modulation frequencies up to 2 MHz, limited by the capabilities of our modulator.

Since the grating formation time of the Cu:KNSBN crystal predicts an amplification bandwidth of 4.3 Hz, we studied the steady-state amplification of signals with phase modulation up to 50 Hz compared to the reference beam. These showed a slight increase in amplification as we increased the modulation frequency from 0 to ~3 Hz,
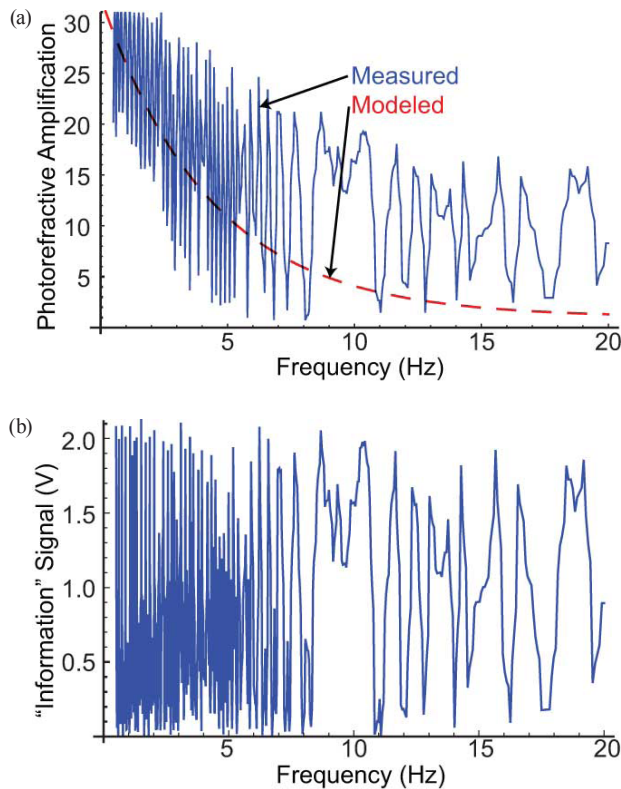
Fig. 8. (a) Photorefractive amplification under phase modulation (blue) has a larger bandwidth than predicted (red) for frequency modulation. (b) The "information" portion of the signal, which is the phase-modulated portion, was amplified approximately evenly over the 20-Hz frequency sweep.
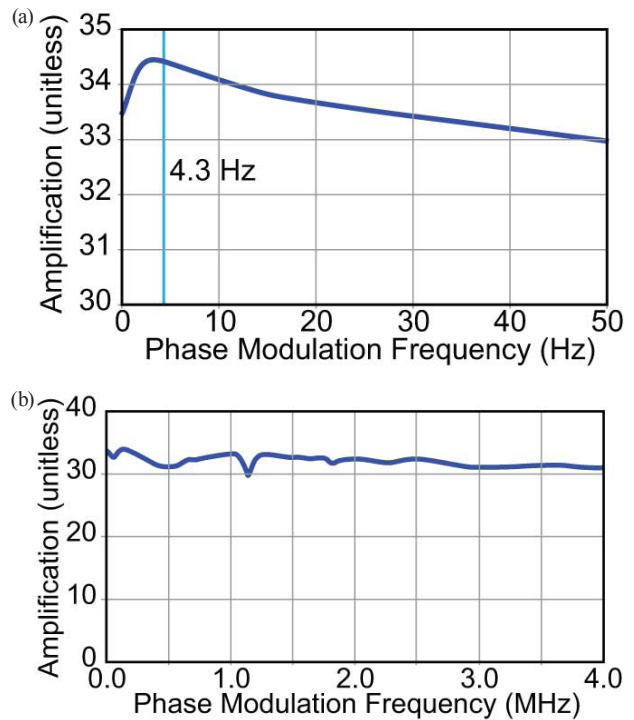
Fig. 9. Photorefractive amplification of phase-modulated signals was constant to within 2.3% over the modulation frequency range dc-50 Hz (a), and to within 8.5% from dc-4 MHz (b).

followed by a slow decline increasing the frequency to 50 Hz (Figure 9(a)). The amplification remained between 33 and 34.5 over this range. It is interesting that at the predicted amplification bandwidth of 4.3 Hz, the amplification is ~2% *higher* than at dc. We then extended our measurements out to a modulation frequency of 4 MHz, and Figure 9(b) demonstrates that the amplification was constant over this range to within 8.5% (and the low point near 1.3 MHz is attributed to an acoustic resonance). We were operating beyond the published limits of our phase modulator at this bandwidth, and could not make accurate measurements at higher frequencies, which will be needed to fully validate our model.

We should note that the Kogelnik model predicts that two beams interfering in an existing volume Bragg grating, at the Bragg angle, would also result in energy transfer from one beam to the other. There would appear to be significant advantages to using a constant Bragg grating as the amplification medium, rather than a photorefractive crystal with its attendant difficulties – slow setup speed, sensitivity to temperature, expense of the nonlinear optical crystal, etc. We can determine the optimum thickness of a Bragg grating directly from Kogelnik's formula for diffraction efficiency, as reproduced in Eq. (5). The optimum thickness can be shown to be

$$d_{opt} = \frac{\lambda}{2\Delta n_e} \frac{\cos\theta}{\cos 2\theta}(1 + 2p) \qquad (16)$$

where *p* is an integer. In the experiment described above, the optimum thickness is 611 μm. This is very thick for a holographic Bragg grating, although permanent custom gratings can be purchased in this thickness. Some higher-order values—3.06 mm, 4.28 mm, and 5.50 mm—are very convenient for photorefractive crystals. There is also a tradeoff between refractive index modulation and optimum thickness; a larger index modulation enables a thinner grating, although this also increases the amplification bandwidth (reducing the SNR gain). For our experiment, the acceptance angle was calculated to be <2 arc minutes. If a permanent volume Bragg grating is used as the energy-transfer medium, the two beams must each be kept in alignment to within half this value. Photorefractive gratings, however, are created by the beams that transfer energy – and automatically remain aligned at exactly the Bragg angle.

The experiments we performed used a signal beam whose intensity was 1.2% that of the reference beam. This is a reasonable approximation to real-world vibrometry for targets several meters away from the illuminator. In longer-range vibrometry, the ratio could easily be much smaller. This results in greater amplification (see Figure 4). The theoretical analysis, however, ignored noise in the photorefractive crystal itself. While the amplification process is noise-free, the gain [Eq. (7)] is dependent on temperature. Our measurements (Figure 7) show random noise whose amplitude is ~5% of the amplified signal, or ~0.1 V. Johnson noise in this region is three orders of magnitude less than this, and gain fluctuations this large would require rapidly fluctuating temperature, so we attribute this to shot noise; we calculate this to be 4% of the total signal in this experiment, in close agreement to the measurements. Our calculations and experiments indicate that the sensitivity of a shot noise-limited photorefractive vibrometer will enable recovery of signals far below the limits of existing vibrometers, almost to the level of the SNR increase inherent in photorefractive amplification.

4. SUMMARY AND CONCLUSIONS

We tested Cu:KNSBN and demonstrated that its photorefractive properties matched well with the STPM. When illuminated at 488.0 nm with a reference beam whose intensity was 8.15 W/cm^2 and a signal beam of intensity 97.8 mW/cm^2, the photorefractive grating formation time was 0.2323 s (rise time from 0 to 1–1/*e*). Ambient temperature was 297K (75.0°F). Used as a photorefractive amplifier, the crystal had a bandwidth of 4.305 Hz (1/0.2323 s) for pure frequency shifts of the signal beam with respect to the reference beam.

Vibrometry, however, measures *phase* modulation rather than frequency shifts. We developed a model of vibration measurement that predicted a much wider amplification bandwidth for phase modulation than frequency modulation. Our model predicts that a target vibrating sinusoidally at ν_0 will produce signals at frequency differences of $\pm 2\nu_0$, $\pm 4\nu_0$,…with the amplitude of the *m*th component falling exponentially with *m*. Most importantly, nearly half the power of the signal will be at zero frequency shift, interfering with the reference beam to produce a standing photorefractive grating and enabling photorefractive amplification at phase modulation frequencies up to hundreds of GHz. We demonstrated that, while single-pass photorefractive amplification fell an order of magnitude for frequency shifts of 20 Hz, amplification of phase modulated signals showed no decline over the same range. We also demonstrated that photorefractive amplification remains nearly constant under these illumination conditions over a bandwidth exceeding 4 MHz.

The application of these results to vibrometry is straightforward. Photorefractive amplification is a field-tested method of increasing an optical signal's intensity up to 80 dB, with fieldable SNR improvements exceeding 40 dB. Since vibrometry measures phase modulation, our experiments demonstrate that photorefractive amplification can significantly enhance measurements of vibrometric signals up to 4 MHz (and much greater, according to the theory), with large signal amplification and significant SNR improvement. This improves vibrometry for targets against bright backgrounds, reduces the power needed for the vibrometric illuminator, and greatly extends the distance at which vibrometric measurements can occur. The self-referencing, self-aligning capabilities of photorefractive amplification also reduce the need for alignment in operation.

References and Notes

1. R. M. Kurtz, A. O. Okorogu, J. Piranian, T. C. Forrester, and T. P. Jannson, *Photorefractive Fiber and Crystal Devices: Materials, Optical Properties, and Applications XI, Proc. SPIE* 6314, 6314O6311 **(2006)**.
2. Z. Zhang, M. Sprenger, M. Gyger, H. J. Eichler, A. Yin, P. Fu, D. Z. Shen, X. Y. Ma, and J. Y. Chen, *Photorefractive Materials: Phenomena and Related Applications II, Proc. SPIE* 3354, 216 **(1998)**.
3. B. F. Pouet, R. K. Ing, S. Krishnaswamy, and D. Royer, *Appl. Phys. Lett.* 69, 3782 **(1996)**.
4. N. V. Kukhtarev, V. B. Markov, S. G. Odulov, M. S. Soskin, and V. L. Vinetskii, *Ferroelectrics* 22, 949 **(1979)**.
5. H. Kogelnik, *Bell Sys. Tech. J.* 48, 2909 **(1969)**.
6. H. Zhang, B. Guo, H. Jiang, Y. Shih, and L. Yan, *App. Phys. B* 61, 207 **(1995)**.
7. J. Quanzhong, L. Xinliang, S. Yongyuan, S. Daliang, and C. Huanchu, *Phys. Rev. B* 50, 4185 **(1994)**.